Passivation Doping

DOI: 10.1002/anie.200904890

# Surface Passivation and Transfer Doping of Silicon Nanowires**

*Chun-Sheng Guo, Lin-Bao Luo, Guo-Dong Yuan, Xiao-Bao Yang, Rui-Qin Zhang,* Wen-Jun Zhang, and Shuit-Tong Lee**

One-dimensional nanomaterials are expected to play a key role in future nanotechnology, in addition to providing model systems to demonstrate the unique characteristics of nanoscale effects. Silicon nanowires (SiNWs) in particular are potentially very attractive, given the central role of Si in the semiconductor industry, and are being extensively studied.[1–3] A SiNW for use in nanodevices is composed of three sections: SiNW core, surface passivant, and adsorbates or interface compounds. A unique way to modulate the transport properties of SiNWs could depend on the individual sections. Volume doping is a conventional method to control conductivity. In volume doping, impurity atoms are introduced into the crystal lattice in the SiNW core by an in situ process during growth,[4,5] ion implantation,[6,7] and related methods. However, volume doping for SiNWs has inherent disadvantages, such as poor controllability and destructive processing. Interestingly, the conductivity of amorphous Si films was found to be sensitive to adsorbates,[8] which indicates the importance of the surface of low-dimensional systems in determining the electrical properties of materials. The large surface-to-volume ratio of SiNWs could potentially be important in influencing their transport properties. Its effect could be exploited through SiNW functionalization. Indeed, recent studies of SiNW-based chemical sensors[9,10] find strong conductivity responses of SiNWs to environmental conditions. Other relevant observations include conductivity modification by adsorbents in the hydrogen-terminated (H-terminated) surfaces of diamond crystals,[11] conductivity determination by surface states in nanoscale thin silicon-on-insulator (SOI) systems,[12] and conductivity enhancement of hydrogenated SiNWs in air and recovery through vacuum or gas purging.[13] Thus, the possibility to modulate the conductivity of SiNWs using surface effects is promising. The ease of such an approach, economically and nondestructively, would offer a unique advantage for use of SiNWs in device fabrication. However, the success of this approach will depend on its controllability and repeatability, and most importantly on the understanding of the mechanisms of the surface effect on SiNWs. Herein, we present a new doping approach, namely surface passivation doping, built on the known surface transfer doping and based on extensive first-principles theoretical investigations and systematic experiments on the surface effects of SiNWs. We also elucidate the involved mechanism and provide better understanding to predetermine the electrical properties of nanomaterials.

Surface hydrogen termination is a natural consequence of the hydrogen fluoride treatment of SiNWs. To reveal the role of hydrogen termination in conductivity, we first performed first-principles calculations based on density functional theory (DFT) with an efficient SIESTA code.[14,15] We adopted popularly used basis sets with double zeta and polarization functions and the Lee–Yang–Parr functional of generalized gradient approximation. We collected atomic charges from a Mulliken population analysis based on DFT calculation, which gave a reasonable charge distribution, as verified using a water molecule ($-0.46\,|e|$ charges on the oxygen atom and $0.23\,|e|$ charges on each hydrogen atom). Interestingly, we obtained extra charges of $-0.06\,|e|$ on average on each surface hydrogen atom of the H-terminated SiNWs (H-SiNWs). Clearly, the partial negative charge on the hydrogen atom is due to the higher electronegativity of the hydrogen atom compared to that of the silicon atom (2.2 vs. 1.9). This partial electron transfer from the silicon core to the surface hydrogen is negligible for bulk silicon but is significant for surface-dominated SiNWs whose carrier concentration could be considerably modified, as is estimated below. Assuming each surface silicon atom is terminated by two hydrogen atoms on average, we can calculate the total number of electrons trapped on the terminating hydrogen atoms using Equation (1):

$$Q = 8q/(a^2 D) \tag{1}$$

where $q$ is the partial charge on a hydrogen atom, $a$ is the silicon lattice constant 5.43 Å, and $D$ is the diameter of the nanowire. For an intrinsic SiNW of 100 nm in diameter and with extra $-0.06\,|e|$ charges at each surface hydrogen atom, around $10^{19}$ $cm^{-3}$ positive charges would be incorporated into the SiNW core near the surface area. Such a high concentration of positive charges (holes) should be detectable in experiments.

To verify the above, we conducted experimental investigations using SiNW arrays synthesized by a chemical etching method.[16] Unlike other as-grown SiNWs with unknown impurities and properties, our as-etched SiNWs inherited well-defined properties from mother silicon wafers, so that they would serve as a model material for the study of surface effects. The typical diameter of the as-etched SiNWs was

[*] C. S. Guo, L. B. Luo, Dr. G. D. Yuan, Dr. X. B. Yang, Dr. R. Q. Zhang, Dr. W. J. Zhang, Prof. S. T. Lee
Center of Super-Diamond and Advanced Films &
Department of Physics and Materials Science
City University Hong Kong, Hong Kong SAR (China)
E-mail: aprqz@cityu.edu.hk
apannale@cityu.edu.hk

[**] This work was supported by grants from the Research Grants Council of Hong Kong SAR [Project No. CityU 103907, CityU5/CRF/08, N_CityU 108/08].

Supporting information for this article is available on the WWW under http://dx.doi.org/10.1002/anie.200904890.

around 100 nm and well above the quantum size region. Their surfaces were cleaned of oxide and terminated with hydrogen by a hydrofluoric acid dip. We fabricated field-effect transistors (FETs) from individual H-SiNWs etched from both n-type and intrinsic silicon wafers and evaluated their electrical characteristics with a Keithley 4200 system in a turbo-pumped high-vacuum system (with a base pressure of $1\times10^{-6}$ Torr). After half an hour at $10^{-6}$ Torr, the current–voltage ($I$–$V$) curve became reproducible as the hydrogenated surface became stable. The results showed that H-SiNWs etched from both intrinsic and n-type silicon wafers invariably exhibited p-type characteristics under high-vacuum conditions. Figure 1a shows the $I_{DS}$–$V_{DS}$ (DS = source–drain)

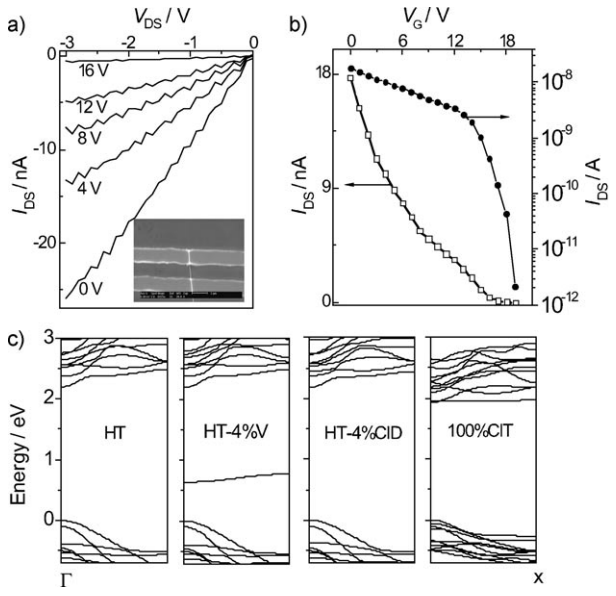


***Figure 1.*** a) $I_{DS}$–$V_{DS}$ curves of a SiNW etched from an intrinsic silicon wafer measured in vacuum at different values of $V_G$. The inset shows an SEM image of the single SiNW FET. b) Linear plot of the transport characteristics at $V_{DS}=-2$ V in vacuum. c) The band structures of ⟨110⟩ SiNWs with hydrogen termination (HT), hydrogen termination with a 4% vacancy (HT-4%V), hydrogen termination with a 4% Cl defect (HT-4%ClD), and 100% Cl termination (100%ClT).

curves of the FET at different gate voltages based on a SiNW etched from an intrinsic silicon wafer at $10^{-6}$ Torr. The inset is a scanning electron microscopy (SEM) image of the single SiNW FET. With the gate voltage $V_G$ modulating the SiNW FET, the $I$–$V$ curves show the typical characteristics of a p-channel semiconductor FET; that is, the conductivity of the SiNW decreases with increasing $V_G$ (and vice versa). Figure 1b depicts the corresponding transport characteristics. For this SiNW of 80 nm in diameter and 2000 nm in length, the resistivity was computed to be 28.9 Ω cm from the $I_{DS}$ versus $V_{DS}$ curve at $V_G=0$ V. Additionally, the hole mobility ($\mu_h$) was calculated from the equation $\mu_h = g_m L^2/C V_{DS}$, where $g_m$ (channel transconductance) is given by $g_m = dI_{DS}/dV_G$ at $1.57\times10^{-9}$ S by fitting the linear part of the $V_G$ versus $I_{DS}$ curve, the channel length $L$ is 2000 nm, and $C$ is the channel capacitance. Assuming a cylindrical shape with an infinite plate model of an SiNW FET, the channel capacitance is given by $C=2\pi\varepsilon_0\varepsilon_r L/\ln(4h/d)$, where $\varepsilon_r$ is the relative dielectric constant of the $SiO_2$ layer, $h$ is the thickness of the dielectric layer, and $d$ is the diameter of the SiNW. Based on these values, $C$ and $\mu_h$ were calculated to be $1.35\times10^{-16}$ F and 0.235 $cm^2V^{-1}s^{-1}$, respectively. The hole concentration was estimated from $\rho=1/(n_h q \mu_h)$ to be $9.6\times10^{17}$ $cm^{-3}$ ($n_h$ = hole concentration, $\mu_h$ = hole mobility). Similar measurements and analysis showed that the SiNW etched from an n-type silicon wafer had in vacuum a mobility of 1.83 $cm^2V^{-1}s^{-1}$ and a calculated hole concentration of $4.1\times10^{17}$ $cm^{-3}$. The experimental results are consistent with the aforementioned theoretical results, thus providing support to our model. Table 1 shows the hole concentrations of the H-SiNWs and the mother or original silicon wafer. However, the minority

***Table 1:*** The hole concentration of the silicon wafer used to prepare H-SiNWs, and the FET-deduced mobility and hole concentration of H-SiNWs in vacuum and in ambient air. The FET hole concentration of the SiNW etched from the intrinsic silicon wafer was larger than that etched from the n-type wafer, because a portion of the holes in the n-type H-SiNWs is compensated by the electrons, whereas such compensation is negligible in the intrinsic SiNWs, with a similar number of electrons being drawn from the core by hydrogen termination.

| | Original Si wafer | In vacuum | | In air | |
|---|---|---|---|---|---|
| | HC[a] | $\mu$[b] | HC[a] | $\mu$[b] | HC[a] |
| H-SiNWs[c] | $1\times10^{9}$ | 0.235 | $9.6\times10^{17}$ | 0.508 | $1.25\times10^{18}$ |
| H-SiNWs[d] | $3.3\times10^{6}$ | 1.83 | $4.1\times10^{17}$ | 4.67 | $7.3\times10^{17}$ |

[a] Hole concentration ($cm^{-3}$). [b] Mobility ($cm^2V^{-1}s^{-1}$). [c] H-SiNWs etched from intrinsic silicon wafer. [d] H-SiNWs etched from n-type silicon wafer.

hole carrier concentrations were only $3.3\times10^{6}$ $cm^{-3}$ in the n-type silicon wafer and $1\times10^{9}$ $cm^{-3}$ in the intrinsic silicon wafer, which are, respectively, eleven and eight orders of magnitude smaller than the hole concentrations of the H-SiNWs at approximately $10^{17}$ $cm^{-3}$.

The huge difference between the carrier concentration of the mother silicon wafer and that of the as-etched SiNWs is striking. Understandably, the surfaces of the as-etched SiNWs from silicon wafers invariably contained some defects, such as impurities and vacancies. Thus, the origin of the hole concentration enhancement needed further verification. We intentionally introduced 4% surface defects into ⟨110⟩ SiNWs of 1.1 to 4 nm in diameter with a reconstructed (100) facet[17] terminated with hydrogen (HT). The effect on the electronic band structure of minority impurities was found to decrease with increasing diameter in our calculations, which is consistent with the report that surface chemical compounds do not exert a noticeable effect until the coverage is larger than 20% in SiNWs larger than 2 nm.[17] Herein, we present only the result of a 1.1 nm SiNW for discussion: 1) hydrogen termination with a 4% vacancy (HT-4%V), that is, one hydrogen atom absent (vacancy); 2) hydrogen termination with a 4% Cl defect (HT-4%ClD), that is, one hydrogen atom replaced by a chlorine atom; and 3) 100% Cl termination (100%ClT), that is, a chlorine-terminated surface. One atom substitution on the surface in our models is equivalent to around a 4% defect. The chlorine defect carries extra −0.21 |

  

e | Mulliken charges, a few times that of the surface hydrogen atom. However, according to Equation (1), electrons trapped in small amounts of chlorine defects, vacancies, or even other impurities will cause only a small change in the hole concentration, compared with $10^{18}$–$10^{19}$ $cm^{-3}$ enhanced by dominant hydrogen termination. The charge transfer between surface passivant and SiNW core is a collective result, because each surface atom is able to trap only a small portion of the charges. Thus, the type of majority carriers in an intrinsic SiNW is dependent on the overall charges trapped in its passivants. Indeed, we found natural p-type conductivity in non-intentionally doped H-SiNWs synthesized by the oxide-assisted growth method[18] and in those with p- or even n-type dopants.[13] Charge trapping plays a dominant role in the effect of surface passivation. Unlike the case of carbon nanotubes,[19] a small amount of surface impurities is expected to have a negligible influence on the band edge of saturated SiNWs, given that the lowest unoccupied molecular orbital (LUMO) and highest occupied molecular orbital (HOMO) are localized in the core.[17] The small amounts of impurities among the main surface passivants are electrically inactive.[20] As shown in Figure 1c, the band structures of HT-4% ClD and HT-4% V for an HT surface remain almost unchanged from those of the perfect HT SiNWs. Although vacancies introduced an isolated deep state into the band gap, such an empty state does not contribute to conductivity. The main features of the band structure and band gap are preserved in the HT-4% V SiNW. However, when the surface defects become dominant, the amount of charge trapped in the surface layer and located at the band edge in band structures of 100% ClT can be modified.[17]

Both the theoretical and experimental investigations showed that carrier concentration in SiNWs is determined by the overall charge transferred between the passivants and the SiNW core. On the basis of this finding, we were able to fabricate nanodevices by simply terminating sections of SiNWs with different passivants to tune conductivity along the wire. For example, we successfully fabricated a p–n junction array with the as-etched SiNWs from n-type doped mother wafers. With SiNWs arrays prepared by the metal-induced HF etching method, oxidization was carried out in a tube furnace at 1150 °C for 4 h in view of the segregating effect of $SiO_2$.[12,21] The oxidized SiNW array was first immersed in a poly(methyl methacrylate) (PMMA) solution, as shown in Figure 2a; afterwards, the top section of the SiNWs was uncovered by etching the PMMA in acetone solution. The oxide sheath of the uncovered section was then removed, and hydrogen termination was introduced. The inset in Figure 2d is a TEM image of the junction area of a typical SiNW, one half of which was hydrogen-terminated and the other half coated with an oxide sheath. After the sectional etching, the bottom wafer was polished and coated with a Ti/Au (60/2 nm) layer. The top end of SiNW array was coated with a layer of Au or Ni thin film for Ohmic contact by electron-beam evaporator, during which the sample was tilted at 60° to avoid metal thin film coating on the junction area. The schematic illustration of the p–n junction setup is shown in Figure 2c. The oxide sheath drew few electrons so that this section of the SiNW retained the n-type conductivity of the

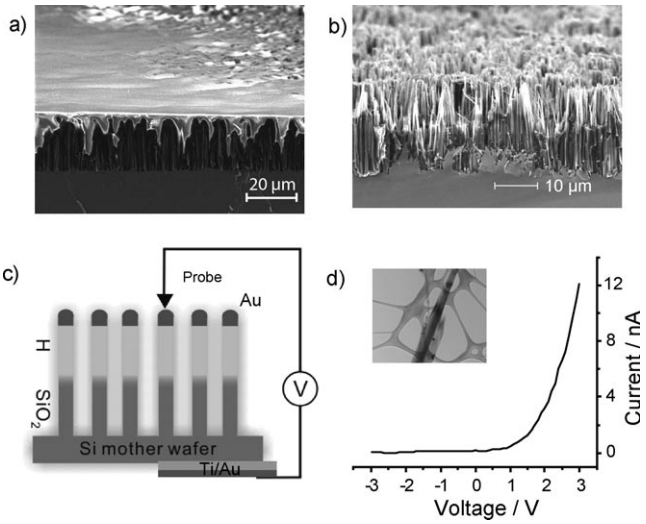


***Figure 2.*** SEM images of a) SiNW arrays fully coated with PMMA photoresist and b) SiNWs partially coated with photoresist and for which the top section is hydrogen-terminated. c) Schematic illustration of the p–n junction. d) The current–voltage characteristics of a p–n junction of a typical SiNW. One half of the wire was hydrogen-terminated and the other half coated with an oxide sheath. The inset shows the TEM image of the junction area, where the bottom section is the part of the SiNW covered with the oxide sheath and the top section is the part with oxide removed using a hydrofluoric acid dip.

mother wafer,[12] whereas the H-terminated section became p-type owing to electron pulling by the terminating hydrogen. By moving the probe to the top end of the SiNW array, the *I*–*V* characteristics of the successfully fabricated p–n junction were measured at room temperature in vacuum, which displays distinctive rectifying behavior with a low turn-on voltage at a forward bias of around 0.8 V, as shown in Figure 2d. The leakage current is less than 0.1 nA at a reverse bias of up to 3 V. Note that there is little or no Schottky barrier with the top contact, as the electrode material is gold, whose work function matches well with that of the p-type silicon nanowire.

The present findings provide insight into previous seemingly conflicting observations. Because of the small electronegativity of silicon, electrons in the SiNW core would similarly be pulled by most nonmetal surface passivants. Cui et al.[22] and Yu et al.[23] reported that, for the same doping levels, B-doped SiNWs had a lower resistance than P-doped SiNWs. However, in doped bulk silicon, the opposite behavior was observed for the same concentration of dopants.[24] This discrepancy could be attributed to trapping of negative charges by surface terminating atoms, which makes p-type doping more efficient than n-type doping in SiNWs.

Moreover, SiNWs and SOI have been found to show strong responses to surface adsorption of various adsorbates or interface compounds.[12,13] Our recent work has shown that the hole concentration of H-SiNWs was enhanced in ambient air.[13] However, the mechanism was unclear. Herein, we also consider theoretically the adsorption of water and other gas molecules on H-SiNWs. Because adsorption is independent of surface orientation on H-SiNWs, we simply chose the (111)

  

surface with a Si–H bond of ⟨112⟩ SiNWs for study. According to our calculations, the weak polar surface Si–H bond enabled weak binding with the electropositive ends of the adsorbed molecules. Specifically, for a water molecule adsorbed on H-SiNWs, the oxygen end of $H_2O$ pointed away from the surface and one of the two hydrogen atoms pointed to the surface hydrogen, forming a dihydrogen bond, as shown in Figure 3a. The calculated $H^{-}\cdots H^{+}$ distance was 1.87 Å with a binding energy of 120 meV per $H_2O$ molecule, which is in good

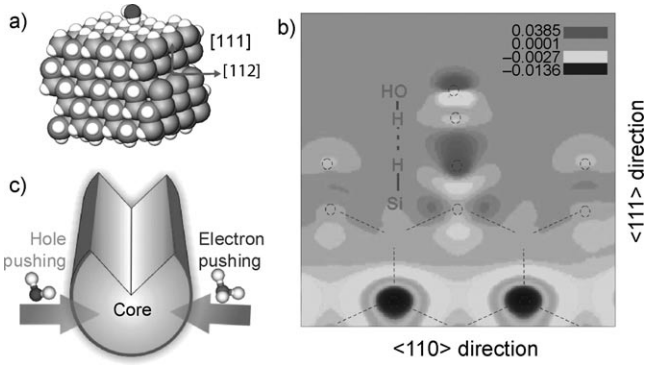


***Figure 3.*** a) The optimized structure of one water molecule absorbed on an H-Si (111) facet. b) Contour map of the $\Delta\rho$ values ($e\,Bohr^{-3}$, see text). The positive area shows electrons gained, while the negative area shows electrons lost. c) The schematic picture of "hole pushing" induced by $H_2O$ adsorbates and "electron pushing" induced by $NH_3$ adsorbates.

agreement with the dihydrogen bonding reported in the literature.[25] This binding energy is in the range of that reported for a dihydrogen bond ($E_b = 50$–$160$ meV), thus indicating a moderate charge transfer in the Si–H bond.

We calculated the charge change of the above H-terminated (111) surface caused by the adsorption of one water molecule using the accurate charge density from the DFT formalism to provide a clear illustration of the charge redistribution. The charge difference shown in Figure 3b is defined as in Equation (2):

$$\Delta\rho = \rho_{\text{HSiNW with water}} - \rho_{\text{HSiNW}} - \rho_{\text{water}} \quad (2)$$

where $\rho$ is the charge density. The positive or negative area shows where electrons are gained or lost, respectively. Clearly, the adsorbed water and the Si–H group gained electrons, whereas the core area lost electrons. The fractional electron was constrained on the water adsorbate and the Si–H group. Based on Mulliken population analysis, the adsorbed water molecule drew $-0.04\,|e|$ (negative charge) from the surface. Each Si–H group carried $-0.08\,|e|$ before or $-0.11\,|e|$ after water adsorption. The SiNW lost additional $0.07\,|e|$, or a fractional positive charge of $0.07\,|e|$ was pushed into the SiNW core. In ambient air, as acidity is generated by $CO_2$, this charge transfer could be even stronger.[24] Consequently, with even a partial coverage of water adsorbates, the hole concentration could be enhanced. The weak binding between the ambient species and the surface Si–H group makes the process reversible under gas purge or vacuum conditions. As shown in Table 1, the SiNW device transferred to the ambient air from vacuum exhibited an increased hole concentration. A series of systematic calculations showed a similar "hole-pushing" mechanism on H-SiNWs, such as for alcohol or acetone adsorption, whereas the adsorption of $NH_3$ showed an opposite effect, an "electron-pushing" process. With the nitrogen end pointing to the surface hydrogen, the $NH_3$ adsorbate carried positive $0.05\,|e|$. The results showed that $NH_3$ adsorption can reduce hole concentration or even convert p-type H-SiNWs into n-type ones. With the valence band maximum (VBM) at $E_v \approx -5.0$ eV and conduction band minimum (CBM) at $E_c \approx -4.2$ eV, H-SiNWs are capable of both donating electrons to and accepting electrons from adsorbates. Therefore, gradual modulations in conductivity may be expected for H-SiNWs through a "hole-pushing" or "electron-pushing" process, as shown in Figure 3c, by depositing acceptor or donor adsorbates, respectively. Indeed, we have observed these kinds of changes in conductivity in recent experiments.[26] Accordingly, SiNWs with other terminations, such as OH or Cl, could also experience considerable influences of adsorbates, while the charge transfer direction might be different.

In summary, first principles calculations and experimental studies revealed doping effects of SiNWs through surface passivation and adsorbates. The large surface-to-volume ratio of SiNWs provides high-efficiency surface modification. Surface effects allow effective doping of SiNWs by electron transfer across the surface layer, which provides a considerable concentration of majority carriers in SiNWs with surface passivants such as hydrogen. Surface passivation doping may be applicable to a wide range of nanodevice applications, including the diode array fabricated herein, through modification of sections of a SiNW with different passivants. Furthermore, the transport properties of SiNWs can be modulated by additional adsorption by transfer of fractional electrons to or from adsorbates. Hence, choosing appropriate chemical compounds for surface passivation and additional adsorption may be a promising alternative approach to conventional volume doping for modulating the conductivity of nanoscale silicon. Our findings also rationalize several experimental results and suggest a unique way to tune the electrical properties of nanomaterials. The generality of the above phenomenon suggests that surface passivation and adsorption may be applicable to modulation of the electrical properties of a wide range of nanomaterials.

Received: May 12, 2009
Revised: September 1, 2009
Published online: December 8, 2009

**Keywords:** adsorption · doping · silicon nanowires · surface passivation · transport properties

[1] Y. Cui, C. M. Lieber, *Science* **2001**, *291*, 851–853.
[2] D. D. D. Ma, C. S. Lee, F. C. K. Au, S. Y. Tong, S. T. Lee, *Science* **2003**, *299*, 1874–1877.
[3] Y. Huang, X. F. Duan, Y. Cui, L. J. Lauhon, K. H. Kim, C. M. Lieber, *Science* **2001**, *294*, 1313–1317.

  

[4] G. F. Zheng, W. Lu, S. Jin, C. M. Lieber, *Adv. Mater.* **2004**, *16*, 1890 – 1893.
[5] Y. Cui, Z. H. Zhong, D. L. Wang, W. U. Wang, C. M. Lieber, *Nano Lett.* **2003**, *3*, 149 – 152.
[6] C. L. Hsin, J. H. He, C. Y. Lee, W. W. Wu, P. H. Yeh, L. J. Chen, Z. L. Wang, *Nano Lett.* **2007**, *7*, 1799 – 1803.
[7] C. Ronning, P. X. Gao, Y. Ding, Z. L. Wang, D. Schwen, *Appl. Phys. Lett.* **2004**, *84*, 783 – 785.
[8] M. Tanielian, H. Fritzsche, C. C. Tsai, E. Symbalisty, *Appl. Phys. Lett.* **1978**, *33*, 353 – 356.
[9] A. Kolmakov, D. O. Klenov, Y. Lilach, S. Stemmer, M. Moskovits, *Nano Lett.* **2005**, *5*, 667 – 673.
[10] F. Patolsky, C. M. Lieber, *Mater. Today* **2005**, *8*, 20 – 28.
[11] M. I. Landstrass, K. V. Ravi, *Appl. Phys. Lett.* **1989**, *55*, 975 – 977.
[12] P. P. Zhang, E. Tevaarwerk, B. N. Park, D. E. Savage, G. K. Celler, I. Knezevic, P. G. Evans, M. A. Eriksson, M. G. Lagally, *Nature* **2006**, *439*, 703 – 706.
[13] J. S. Jie, W. J. Zhang, K. Q. Peng, G. D. Yuan, C. S. Lee, S. T. Lee, *Adv. Funct. Mater.* **2008**, *18*, 3251 – 3257.
[14] P. Ordejón, E. Artacho, J. M. Soler, *Phys. Rev. B* **1996**, *53*, R10441 – R10444.
[15] D. Sanchez Portal, P. Ordejon, E. Artacho, J. M. Soler, *Int. J. Quantum Chem.* **1997**, *65*, 453 – 461.
[16] K. Q. Peng, Y. Wu, H. Fang, X. Y. Zhong, Y. Xu, J. Zhu, *Angew. Chem.* **2005**, *117*, 2797 – 2802; *Angew. Chem. Int. Ed.* **2005**, *44*, 2737 – 2742.
[17] P. W. Leu, B. Shan, K. J. Cho, *Phys. Rev. B* **2006**, *73*, 195320.
[18] R. Q. Zhang, Y. Lifshitz, S. T. Lee, *Adv. Mater.* **2003**, *15*, 635 – 640.
[19] P. G. Collins, K. Bradley, M. Ishigami, A. Zettl, *Science* **2000**, *287*, 1801 – 1804.
[20] M. V. Fernández-Serra, C. Adessi, X. Blase, *Phys. Rev. Lett.* **2006**, *96*, 166805.
[21] G. Dubey, G. P. Lopinskia, F. Rosei, *Appl. Phys. Lett.* **2007**, *91*, 232111.
[22] Y. Cui, X. F. Duan, J. T. Hu, C. M. Lieber, *J. Phys. Chem. B* **2000**, *104*, 5213 – 5216.
[23] J. Y. Yu, S. W. Chung, J. R. Heath, *J. Phys. Chem. B* **2000**, *104*, 11864 – 11870.
[24] S. M. Size, *Physics of semiconductor devices*, Wiley, New York, **1981**.
[25] R. Custelcean, J. E. Jackson, *Chem. Rev.* **2001**, *101*, 1963 – 1980.
[26] G. D. Yuan, Y. B. Zhou, C. S. Guo, W. J. Zhang, Y. B. Tang, Y. Q. Li, Z. H. Chen, P. F. Wang, R. Q. Zhang, I. Bello, C. S. Lee, S. T. Lee, unpublished results.

  